Communications

Sequential Organic−Inorganic Templating and Thermoelectric Properties of High-Aspect-Ratio Single-Crystal Lead Telluride Nanorods

Arup Purkayastha,[†] Qingyu Yan,[†] Darshan D. Gandhi,[†] Huafang Li,[†] Gyana Pattanaik,[†] Theodorian Borca-Tasciuc,[‡] N. Ravishankar,[§] and G. Ramanath*,[†]

Department of Materials Science and Engineering and Department of Mechanical Aerospace and Nuclear Engineering, Rensselaer Polytechnic Institute, Troy, New York 12180, and Materials Research Centre, Indian Institute of Science, Bangalore 560012, India

Received November 5, 2007
Revised Manuscript Received May 19, 2008

Chalcogenides such as bismuth telluride and lead telluride exhibit high thermoelectric figures of merit ZT[1–3] in the bulk because of a combination of high electrical conductivity σ and Seebeck coefficient S, and low thermal conductivity κ, making them attractive for refrigeration and generating electrical power from heat.[4–6] Nanostructuring these materials along one dimension (e.g., nanolayers) has been shown to increase ZT because of size and quantum effects on S, σ, and κ.[7,8] Greater degrees of confinement (e.g., PbTe nanowires with characteristic dimensions <5 nm)[9] are expected to provide higher ZT increases and open up entirely new types of possibilities for novel applications such as cooling nanoscale hotspots in nanodevice interconnections comprising nanowires or nanotubes and creating nanoscale power generators.

Growing one-dimensional nanocrystals of chalcogenides with a cubic crystal structure (e.g., PbTe, rocksalt structure) is a challenge because of the necessity of a symmetry-breaking pathway for enabling anisotropic growth.[10] Solvothermal decomposition or polyol reduction yield spherical[11] or cube-shaped[12,13] nanoparticles. Incorporating surfactants provides particle size control, but is ineffective in inducing shape anisotropy because of the high crystallographic degeneracy in cubic crystals. Alternative methods based on oriented attachment of nanoparticles in solution,[14–16] catalyst-mediated vapor−liquid−solid reactions,[17,18] and inorganic templating have been devised.[19,20] However, nanowire polycrystallinity and template removal issues limit the utility of these routes for fundamental studies and for reaping the maximal benefit of the properties of single crystals for applications. Recently devised sonochemical and autoclave-based techniques,[21–23] e.g., <10 nm diameter nanorods[12] with aspect ratios $\lesssim$7, and formation of single-crystal nanowires through nanoparticle coalescence and ripening, however, are promising approaches.[31]

Here, we report a completely new two-step organic−inorganic templating method to obtain single-crystal PbTe nanorods with aspect ratios up to 27, at moderate temperatures, without using an autoclave. We exploit anisotropic nanotube growth through organic surfactant templating and transform the nanotubes into single-crystal PbTe nanorods via reaction with a lead salt obviating any subsequent template removal. Nanorod to nanotube conversion has been reported,[25] but the reverse process reported here is new and can be applied to producing anisotropic nanostructures of materials with a cubic structure.

In the first step, Te nanotubes were synthesized by solvothermal reduction of TeO_2 in the presence of cetyl ether,

* Corresponding author. E-mail: ramanath@rpi.edu.
[†] Department of Materials Science and Engineering, Rensselaer Polytechnic Institute.
[‡] Department of Mechanical Aerospace and Nuclear Engineering, Rensselaer Polytechnic Institute.
[§] Materials Research Centre, Indian Institute of Science.

(1) Goldsmid, H. J. *Thermoelectrc Refrigeration*; Plenum: New York, 1964.
(2) Heremans, J. P.; Thrush, C. M.; Morelli, D. T. *Phys. Rev. B* **2004**, *70*, 115334.
(3) Purkayastha, A.; Kim, S.; Gandhi, D. D.; Ganesan, P. G.; Borca-Tasciuc, T.; Ramanath, G. *Adv. Mater.* **2006**, *18*, 2958.
(4) Poudeu, P. F.P.; D'Angelo, J.; Kong, H.; Downey, A.; Short, J. L.; Pcionek, R.; Hogan, T. P.; Uher, C.; Kanatzidis, M. G. *J. Am. Chem. Soc.* **2006**, *128*, 14347.
(5) Rowe, M. D., *CRC Handbook of Thermoelectrics*; CRC Press: Boca, Raton, FL, 1995.
(6) Zogg, H.; Kellermann, K.; Alchalabi, K.; Zimin, D. *Infrared Phys. Technol.* **2004**, *46*, 155.
(7) Venkatasubramanian, R.; Siivola, E.; Colpitts, T.; O'Quinn, B. *Nature* **2001**, *413*, 597.
(8) Chen, G.; Dresselhaus, M. S.; Dresselhaus, G.; Fleurial, J. P.; Caillat, T. *Int. Mater. Rev.* **2003**, *48*, 45.
(9) Hicks, L. D.; Harman, T. C.; Sun, X.; Dresselhaus, M. S. *Phys. Rev. B* **1996**, *53*, R10 493.
(10) Halder, A. and Ravishankar, N. *Adv. Mater.* **2007**, *18*, 1854.
(11) Murphy, J. E.; Beard, M. C.; Norman, A. G.; Ahrenkiel, S. P.; Johnson, J. C.; Yu, P.; Micic, O. I.; Ellingson, R. J.; Nozik, A. J. *J. Am. Chem. Soc.* **2006**, *128*, 3241.
(12) Wang, W.; Poudel, B.; Wang, D.; Ren, Z. F. *Adv. Mater.* **2005**, *17*, 2110.
(13) Poudel, B.; Wang, W. Z.; Wang, D. Z.; Huang, J. Y.; Ren, Z. F. *J. Nanosci. Nanotechnol.* **2006**, *6*, 1050.
(14) Tang, Z.; Kotov, N. A.; Giersig, M. *Science* **2002**, *297*, 237.
(15) Cho, K. S.; Talapin, D. V.; Gaschler, W.; Murray, C. B. *J. Am. Chem. Soc.* **2005**, *127*, 7140.
(16) Yu, J. H.; Joo, J.; Park, H. M.; Baik, S.; Kim, Y. W.; Kim, S. C.; Hyeon, T. *J. Am. Chem. Soc.* **2005**, *127*, 5662.
(17) Hannon, J. B.; Kodambaka, S.; Ross, F. M.; Tromp, R. M. *Nature* **2006**, *440*, 69.
(18) Duan, X.; Lieber, C. M. *Adv. Mater.* **2000**, *12*, 298.
(19) Xu, D.; Chen, D.; Xu, Y.; Shi, X.; Guo, G.; Gui, L.; Tang, Y. *Pure Appl. Chem.* **2000**, *72*, 127.
(20) Fan, H. J.; Werner, P.; Zacharias, M. *Small* **2006**, *2*, 700.
(21) Zou, G.; Liu, Z.; Wang, D.; Jiang, C.; Quian, Y. *Eur. J. Inorg. Chem.* **2004**, 4521.
(22) Qiu, X.; Lou, Y.; Samia, A.C. S.; Devadoss, A.; Burgess, J. D.; Dayal, S.; Burda, C. *Angew. Chem., Int. Ed.* **2005**, *44*, 5855.
(23) Zhang, L.; Yu, J. C.; Mo, M.; Wu, L.; Kwong, K. W.; Li, Q. *Small* **2005**, *1*, 349.
(24) S Cho, K.; Talapin, D. V.; Gaschler, W.; Murray, C. B. *J. Am. Chem. Soc.* **2005**, *127*, 7140.
(25) Tong, H.; Zhu, Y-J.; Yang, L-X.; Li, L.; Zhang., L. *Angew. Chem., Int. Ed.* **2006**, *45*, 7739.

10.1021/cm703158f CCC: $40.75
Published on Web 07/04/2008

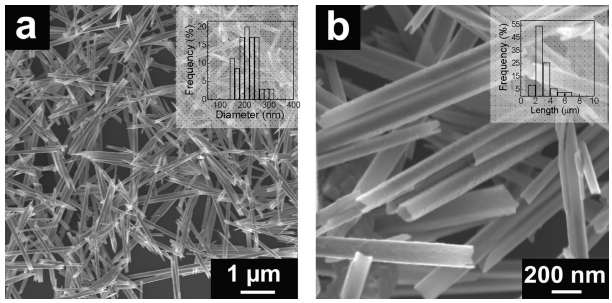

Figure 1. Representative (a) low- and (b) high-magnification SEM micrographs of Te nanotubes synthesized from TeO_2 with 1.5 mmol brij 52 and 0.5 mmol L-lysine ethyl ester dihydrochloride. Insets show the diameter and length distributions of the Te nanotubes.

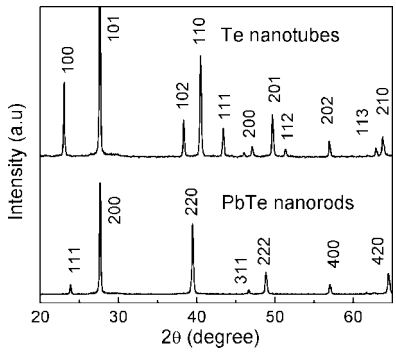

Figure 2. X-ray diffractograms obtained from Te nanotubes and PbTe nanorods showing Bragg peaks corresponding to trigonal Te with lattice parameters $a = 0.446$ nm and $c = 0.593$ nm (top), and cubic PbTe with a rocksalt structure and lattice parameter $a = 0.646$ nm (bottom).

a nonionic surfactant brij 52, and L-lysine ethyl ester dihydrochloride, an ionic surfactant. This route is similar to a previously reported method,[26] except that our method uses two shape-directing surfactants to form nanotubes at a lower temperature, without an autoclave.[27] In a typical synthesis, 1.5 mmol brij 52 and 0.5 mmol L-lysine ethyl ester dihydrochloride were added to preheated ethylene glycol at 140 °C, followed by TeO_2 addition and refluxing for 5 h. The Te nanotubes are cylinder-shaped, straight, and faceted (see Figure 1a). High-magnification images (see Figure 1b) reveal hollow cylinders with a hexagonal cross-section, and an average diameter and length of 210 ± 40 nm and 2730 ± 40 nm, respectively (see insets in images a and b in Figure 1). Extensive SEM examination of several samples did not reveal nanostructures of any other shape (particles, cubes, etc.), indicating a high degree of shape selectivity.

X-ray diffractograms show that the Te nanotubes have a trigonal crystal structure (see Figure 2). We attribute Te nanotube formation to L-lysine ethyl ester dihydrochloride, consistent with the promotion of anisotropic Te growth by lysine.[28] TeO_2 reduction without brij 52 results in Te nanowires without the hollow, indicating that brij 52 templates the hollow, probably in a way similar to templating hexagonal pore arrays in silica.[29]

The Te nanotube solution was cooled to 100 °C and mixed with aqueous $PbCl_2$. Drop-by-drop addition of hydrazine monohydrate reduces $PbCl_2$ and transforms the Te nanotubes to single-crystal PbTe nanorods, as described below. X-ray diffractograms from Te nanotubes treated with Pb^{2+} and hydrazine show a lone set of Bragg peaks corresponding to cubic PbTe. The higher (222) Bragg intensity compared to that of (111) confirms the rocksalt structure (see Figure 2).

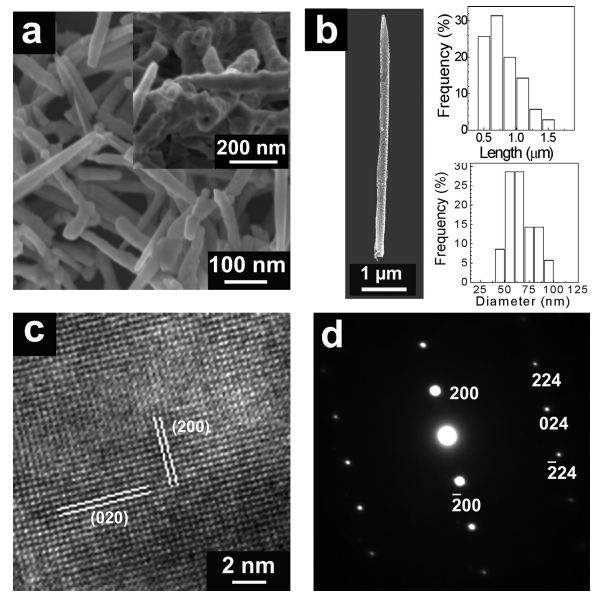

Figure 3. Representative (a) SEM image of PbTe nanords. Inset in (a) illustrates a decrease in inner nanotube diameter and increase in tube wall thickness. (b) TEM image of 5-μm-long PbTe nanorod obtained by manipulating the reaction conditions along with diameter and length distributions of the nanorods. (c) High-resolution TEM image of a nanorod taken along the [002] zone. (d) Electron diffraction pattern from an individual PbTe nanorod taken along the [02$\bar{1}$] zone.

Panels a and b in Figure 3 show that PbTe retains the one-dimensional shape of Te nanotubes, except for a decrease and disappearance of the hollow. Figure 3a inset provides an end-on view of the PbTe nanorods with a remnant hollow with a decreased diameter. This, and the lack of observation of low-aspect-ratio nanostructures such as particles or cubes of PbTe or other compounds in our samples (within the sensitivity limits of our diffraction microscopy and spectroscopy analyses) indicate that nanorod formation by the Pb^{2+} reduction by hydrazine inside the nanotube surface is preferred over precipitation of lead particles or Te leaching.

The mean nanorod diameter and length (66 ± 12 nm and 713 ± 50 nm, respectively, see histograms in Figure 3b), are 3-fold smaller than the parent Te nanotubes, and 2-fold smaller than mass-balance estimates assuming bulk densities and complete conversion of the Te nanotubes. The reason for radial shrinkage is not clear, but tube breakage during surfactant removal by repeated sonication could be a contributor for length decrease.[25]

High-resolution TEM images and selected-area electron diffraction patterns (see panels c and d in Figure 3) show that each PbTe nanorod is a single crystal, oriented along the [100] direction of the rocksalt structure. Energy-dispersive X-ray spectra from the nanorods reveal the nanorod composition to be within ±4% of the $Pb_{0.5}Te_{0.5}$ stoichiometry, consistent with the Pb/Te salt ratio (see the Supporting Information, Figure S3).

The importance of the preformed Te nanotubes for single-crystal PbTe nanorod formation is underscored by the

(26) Mayers, B.; Xia, Y. *Adv. Mater.* **2002**, *14*, 279.
(27) Xi, G.; Peng, Y.; Yu, W.; Quian, Y. *Cryst. Growth Des.* **2005**, *5*, 325.
(28) He, Z.; Yu, S-H.; Zhu, J. *Chem. Mater.* **2005**, *17*, 2785.
(29) Dattelbaum, A. M.; Amweg, M. L.; Ecke, L. E.; Yee, C. K.; Shreve, A. P.; Parikh, A. N. *Nano Lett.* **2003**, *3*, 719.

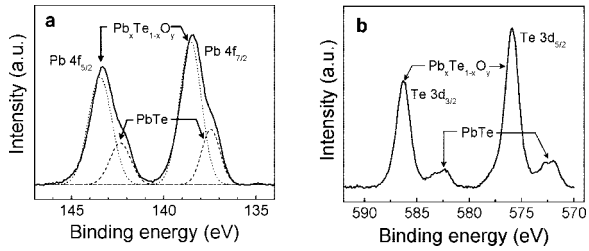

Figure 4. Core-level spectra of (a) Pb 4f and (b) Te 3d states acquired from PbTe nanorods dispersed on a Au surface. In (a), the dashed sub-bands denote unoxidized PbTe, whereas the dotted curves denote oxidized PbTe.

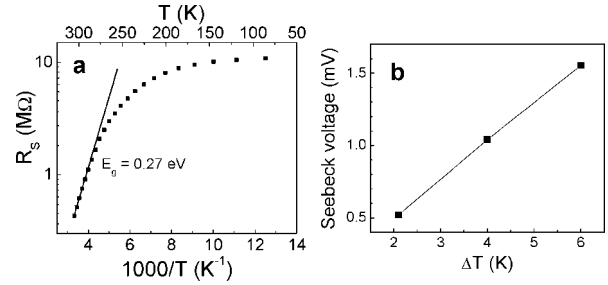

Figure 5. (a) A semilog plot of electrical resistance of a thin film of PbTe nanorods as a function of inverse of temperature. (b) Seebeck voltage as a function of the temperature difference ΔT between two thermocouples placed 2 mm apart on the film of PbTe nanorods.

formation of isotropic PbTe nanostructures when Pb and Te salts were reduced directly by hydrazine hydrate in the presence of brij 52 and L-lysine ethyl ester dihydrochloride. In this baseline experiment, there were only traces (<5%) of nanorod-like structures (see the Supporting Information, Figure S1). This result also indicates that brij 52 and L-lysine ethyl ester dihydrochloride do not directly promote the anisotropic growth of PbTe. The PbTe nanorod dimensions can be tuned by adjusting the brij 52 concentration during Te nanotube synthesis. Nanorod size increases with brij 52 content; the length rate increase is slightly larger than the diameter increase rate (see the Supporting Information, Figure S2). For example, increasing the brij 52 content from 1.5 to 3 mmol increases the PbTe nanorod aspect ratio from ~7−17 to ~8−27. Several-micrometer-long PbTe nanorods are obtainable (see Figure 3b) by slow reduction of Pb salts at 100 °C followed by reduction at 180 °C.

Core-level spectra from the PbTe nanorod samples show both unoxidized and oxidized forms of PbTe (see Figure 4). The Pb $4f_{7/2}$ sub-band at 138.5 eV and the dual Te 3d sub-bands at 571.9 and 582.3 eV correspond to unoxidized PbTe.[30] The high-energy Pb 4f sub-band at 143.4 eV and the Te 3d chemical states at 575.9 and 586.2 eV are from oxidized PbTe. The oxidized band component is greater, as expected, beacause our synthesis was in a non-inert atmosphere. The presence of unoxidized PbTe signatures suggests that the oxide is likely restricted only to the nanorod surface with a thickness less than Pb 4f and Te 3d electron escape depths (<2 nm). The oxidized-PbTe/unoxidized-PbTe sub-band intensity ratio increases with reaction time: from 2.6 in 5 h, to 8.4 for 24 h (see the Supporting Information, Figure S4), and with decreasing hydrazine concentration.

We measured the electrical sheet resistance R_S and Seebeck coefficient S of a thin film assembly of PbTe nanorods by dip coating a nanostructure solution onto a glass substrate patterned with Au electrodes and a microfabricated heater. The average PbTe nanorod diameter in the thin film assembly was 66 ± 12 nm. Prior to our measurements, the thin film assembly of the nanorods was exposed to hydrazine for 4 h to partially reduce the surface oxide and improve internanostructure contact. Figure 5a is a semilog plot of electrical resistance of PbTe nanorods film as a function of inverse of temperature. The linear region in the vicinity of room temperature connotes an energy gap of 0.27 eV for the PbTe nanorod film, which is slightly less than the value for bulk PbTe. At lower temperatures the resistance is higher, and shows weaker temperature dependence as reported for PbTe thin films.[31] This temperature-independent carrier transport is reminiscent of internanostructure carrier tunneling.[32] However, near room temperature, carrier generation within the nanostructure becomes the major mechanism limiting the transport. The Seebeck voltage measured between two points on the nanorod thin film assembly varies linearly with temperature (see Figure 5b), yielding a room-temperature Seebeck coefficient $S = 263\ \mu$V/K, which is in the range of the reported value of 265 μV/K for bulk PbTe and that reported for PbTe nanocrystalline films.[33,34] This result suggests that the electrical transport in the investigated nanostructures is similar to bulk behavior.

In summary, we have demonstrated a new two-step organic−inorganic templating route to synthesize high aspect ratio PbTe nanorods from Te nanotubes. The nanorod aspect ratio can be tailored by changing the reaction temperature and cetyl ether concentration.Our technique could also be potentially adapted to synthesize one-dimensional nanostructures of other metal chalcogenides. The Seebeck coefficient of dip-coated nanorods film is promising. Further studies are necessary to unveil the electrical and transport mechanisms in individual nanostructures and their junctions. We anticipate that the high aspect ratio of the PbTe nanorods synthesized here, and their amenability to be assembled into thin films, would be attractive for fabricating novel thermoelectric devices.

Acknowledgment. We gratefully acknowledge support from the Interconnect Focus Center funded by MARCO and NY State, and the National Science Foundation under Grants ECS 0501488, DMR 0519081, and CTS 0348613.

Supporting Information Available: Experimental details and additional figures (PDF). This material is available free of charge via the Internet at http://pubs.acs.org.

CM703158F

(30) Zyubina, T. S.; Neudachina, V. S.; Yashina, L. V.; Shtanov, V. I. *Surf. Sci.* **2005**, *574*, 52.
(31) Todoroki, S.; Onuma, Y. *Jpn. J. Appl. Phys.* **1975**, *14*, 466.
(32) Sze, S. M. *Physics of Semiconductor Devices*; Wiley: New York, 1981.
(33) Heremans, J. P.; Thrush, C. M.; Morelli, D. T. *Phys. Rev. B* **2004**, *70*, 115334.
(34) Dashevsky, Z.; Kreizman, R.; Dariel, M. P. *J. Appl. Phys.* **2005**, *98*, 094309.